

Reducing the effects of specular scatterers on QUS imaging using the generalized spectrum

Adam Luchies, Goutam Ghoshal, William D. O'Brien, Jr., Michael L. Oelze
 Bioacoustics Research Laboratory, Department of Electrical and Computer Engineering
 University of Illinois at Urbana-Champaign
 Urbana, Illinois, 61820
 Email: luchies1@illinois.edu

Abstract—The effective scatterer diameter (ESD) and effective acoustic concentration (EAC) are quantitative ultrasound (QUS) imaging parameters that employ scattering models and spectral fit methods to characterize tissue microstructure. These methods work best when the region of interest (ROI) from which the parameters are derived contains uniform diffuse scatterers. In some tissues, specular scatterers (e.g., calcifications, blood vessels, etc.) can exist and cause decreases in the accuracy and precision of QUS parameter estimates based on diffuse scattering.

In this study the generalized spectrum (GS) intercept parameter was used to detect echoes from specular scatterers. The signals corresponding to the specular scatterers were then removed in order to reduce the effect of specular scatterers on QUS estimates. Backscatter data from a simulated phantom, rat mammary tumors, and fresh beef liver samples that underwent elevations in temperature were analyzed to evaluate the effectiveness of using the GS intercept parameter. The ESD and EAC were estimated assuming a spherical Gaussian scattering model for each data block outlined in an ROI in the sample. The GS intercept parameter was estimated for each data block and used to sort data blocks and their corresponding QUS estimates were sorted into diffuse and specular scattering groups. Modified parametric images were then formed by using only the data blocks in the diffuse scattering group.

For the simulated phantom, the exclusion of specular scatterers from the QUS estimates resulted in a reduction in ESD standard deviation of 66.4%. For the rat mammary tumors, the average reduction in ESD and EAC standard deviation was 17.1% and 24.8%, respectively. When monitoring the changes in ESD and EAC in beef liver samples versus temperature over the temperature range of 37 to 50 °C, the mean ESD and EAC values changed monotonically with temperature. By excluding the specular scatterers, ESD and EAC were observed to change by 25.4% and -40.3% respectively as opposed to 14.8% and -30.7% respectively when including specular scatterers. When excluding specular scatterers from QUS analysis, the precision of QUS estimates was improved and the sensitivity of QUS estimates to temperature changes was increased. These results suggest that the GS intercept parameter has the potential to reduce the effects of specular scatterers on diffuse scattering estimates and to improve QUS imaging.

Keywords—generalized spectrum; quantitative ultrasound; specular scatterers; ultrasound backscatter

I. INTRODUCTION

Quantitative ultrasound (QUS) techniques have been developed as a means to detect and diagnose cancer in the breast, prostate, and eye [1-3]. The effective scatterer diameter (ESD) and effective acoustic concentration (EAC) are examples of model-based QUS parameters that have the potential to accomplish this task [1]. The ESD and EAC result from parameterizing the power spectral estimate from ultrasound backscatter for a data block corresponding to a location in tissue. These QUS estimates have been linked to information related to tissue microstructure. The power spectral estimate is formed by averaging spectra from adjacent and independent scan lines within the data block. Averaging in this manner requires the assumption that the data block contains uniform diffuse scattering. In some tissues, specular scatterers (i.e., single dominant scatterers or coherent scatterers) can exist and invalidate the assumption of uniform diffuse scattering. Although the existence of these specular scatterers can provide diagnostically useful information, they can also decrease the accuracy and precision of QUS estimates based on diffuse scattering. The goal of this work was to detect echoes from specular scatterers in order to create QUS images based on diffuse scattering only.

II. METHODS

A. Generalized Spectrum

One method to detect specular scatterers in tissue is to estimate the generalized spectrum (GS) [4] of the ultrasound backscattered signal. The GS detects the spectral correlation between different frequency components that is produced by a specular scatterer in the frequency domain representation of the backscattered signal. This spectral correlation between different frequency components is small for diffuse scattering. The generalized spectrum for a radiofrequency (RF) signal segment $y(t)$ is defined over the bifrequency plane and is given by:

$$G(f_1, f_2) = E \left[Y(f_1) Y^*(f_2) \right] \quad (1)$$

where $Y(f)$ is the Fourier transform of $y(t)$ and the superscript * represents a complex conjugate. The discrete generalized spectrum can be estimated for a data block using a synchronized time-averaging method given by [4]:

$$\hat{G}(f_1, f_2) = \frac{1}{N} \sum_{n=1}^N Y_i(f_1) e^{j2\pi f_1 \tau_i} \times Y_i^*(f_2) e^{-j2\pi f_2 \tau_i} \quad (2)$$

where N is the total number of segments in the data block used to estimate the GS, $Y_i(f)$ is the Fourier transform of the i th scan line, and τ_i is the synchronization constant for the i th scan line. The synchronization constant aids in GS convergence when specular or periodic scatterers are present. The collapsed average (CA) over the generalized spectrum allows for extraction of useful parameters and is given by [4]:

$$\hat{C}(f') = \frac{1}{M(f')} \sum_{f_2 - f_1 = f'} \hat{G}(f_1, f_2) \quad (3)$$

where f' is the frequency difference associated with the off diagonal components of the bifrequency plane and $M(f')$ is the total number of discrete GS points associated with the off-diagonal component $f_1 - f_2 = f'$. The collapsed average is normalized by its maximum value and displayed on a logarithmic scale for linear regression analysis. The y-intercept parameter (referred to as the GS intercept parameter from this point forward) of the best-fit line to the collapsed average increases in value when specular scattering is present in a data block compared to when only diffuse scattering is present.

B. Simulation

Simulations were used to study the effects of detecting and removing specular scatterers from QUS analysis via the GS intercept parameter. A simulated backscatter phantom was generated in MATLAB with diffuse scatterers (7 scatterers/resolution cell) and specular scatterers (1 scatterer/cc) using a spherical Gaussian model. Diffuse scatterers were simulated using a size of 50 μm and specular scatterers simulated using a size of 100 μm . The specular scatterers had scattering signal amplitude five times that of the diffuse scatterers. The phantom was assumed to be acoustically lossless. The source impulse response was modeled by a modulated Rayleigh pulse having a center frequency of 10 MHz and -6-dB pulse/echo bandwidth of 5 MHz. Scan lines were constructed by linearly combining the scattered pulse due to the incident pulse from each individual scatterer location in the beam field. Multiple scan lines were constructed by translating the simulated transducer laterally across the length of the phantom.

C. Experimental methods

Experimental backscatter data were analyzed from two types of tissues using the GS intercept parameter. First, ultrasonic backscatter data from rats that had spontaneously developed mammary tumors (fibroadenomas) were analyzed. Tumors ranged in size from one to six cm in diameter. The

animal was mounted in a custom designed holder that allowed direct access to the tumor site. The animal was euthanized and placed in a tank of degassed room temperature water for scanning. A focused transducer with a nominal center frequency of 7.5 MHz (f-number=4) and a -6 dB frequency bandwidth of 6 MHz was used to scan the tumors. The transducer was moved using a computer-controlled micro-positioning system while the sample was held stationary. A total of five, two-dimensional B-mode slices (a scan line spacing of 150 μm was used) separated by 1 mm were acquired for each animal. After the scans, the tumors were excised, fixed in formalin, trimmed for histology, and sent for pathology. For this study, all of the analyzed tumors were fibroadenomas and only tumor slices with at least one specular scatterer on the interior region of the tumor were analyzed. Reference scans were acquired for the transducer from a Plexiglas reflector, using the same equipment settings as for the tumor imaging.

Second, experimental backscatter was analyzed from six fresh beef liver samples scanned at temperatures ranging from 37 to 50°C in 1°C increments. Multiple specular scatterers were noticeable in the beef livers, possibly due the presence of blood vessels. The samples were completely submerged in 0.9% saline solution made from degassed water and a 20-MHz single-element f/3 transducer with -10 dB bandwidth of 18 MHz was used for scanning. The transducer was moved using a computer-controlled micro-positioning system while the sample was held stationary. A total of 30 adjacently spaced scan lines with a lateral step size of 200 μm (approximately one full beamwidth) were collected for each sample and each temperature. A mechanical coil heater was used to heat the water bath and liver sample. A needle thermocouple (Omega Engineering, Inc., Stamford, CT) was placed within the samples and was used to monitor the temperature in the samples with an accuracy of 0.1 °C. Backscatter was collected at every 1°C increase in temperature. Sound speed and attenuation were estimated versus temperature using an insertion loss method. Reference scans were acquired for the transducer from a Plexiglas reflector, using the same equipment settings as for the tumor imaging.

D. Data Analysis

In each sample, the area for QUS analysis was manually marked and divided into small overlapping data blocks. The backscatter coefficient (BSC) was estimated for each data block. The ESD and EAC parameters were measured by assuming a spherical Gaussian model and selecting parameters to minimize the mean square error between theoretical BSC and experimental BSC [5]. The GS intercept parameter was estimated for each data block and then used to sort data blocks (and their corresponding QUS estimates) into diffuse and specular scattering groups. For the simulated phantom and rat mammary tumors, the standard deviations of the ESD and EAC were computed by including all data blocks and then compared to the standard deviations of the ESD and EAC computed by including only the data blocks in the diffuse scattering group. For the beef liver tissue, QUS sensitivity to temperature was estimated by computing the percent change in ESD and EAC mean values at a particular temperature with respect to the initial ESD and EAC mean values at 37°C.

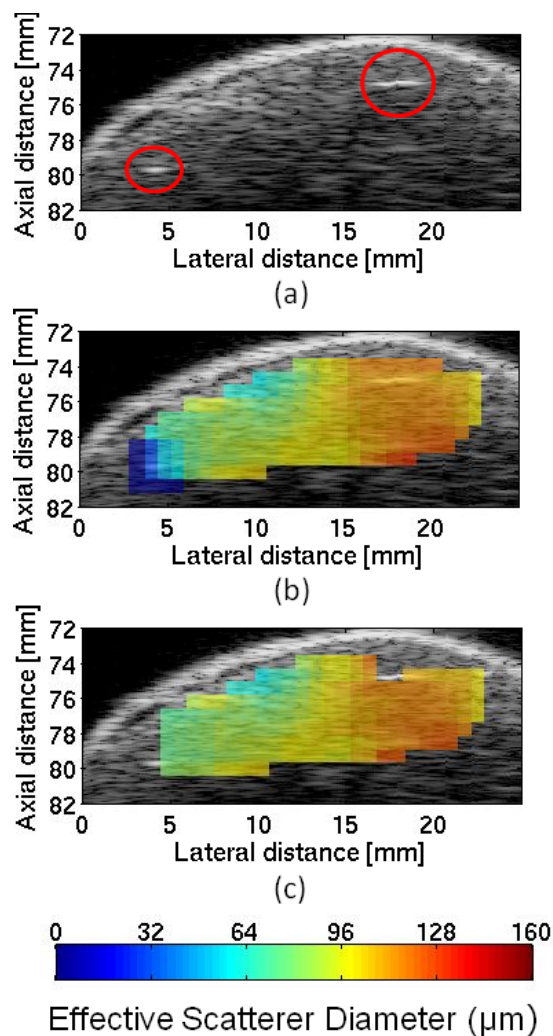


Figure 1. Example of rat mammary tumor (a) B-mode image, (b) ESD parametric image overlay when including specular scatterers, (c) ESD parametric image overlay when excluding specular scatterers.

III. RESULTS

For the simulated phantom, when all data blocks were included in the analysis (i.e., specular scatterers were included), the ESD estimate mean and standard deviation were $60.3 \pm 18.2 \mu\text{m}$. When only the data blocks from the diffuse scattering group were used (i.e., specular scatterers were excluded), the ESD estimate mean and standard deviation were $50.1 \pm 6.1 \mu\text{m}$.

A total of six rat mammary tumors were included in the analysis. Two slices taken at different positions were included from four of the tumors, thus providing 10 independent backscatter slices. An example of a rat mammary tumor with several specular scatterers is shown in Fig. 1a. An example of the effect on the ESD parametric image overlay when excluding specular scatterers can be observed in Figs. 1b. and 1c. The effect on ESD and EAC estimate standard deviations for the rat mammary slices can be observed in Fig. 2. The average percent reduction in ESD and EAC standard deviations for all rat mammary slices when specular scatterers were excluded was 17.1% and 24.8% respectively.

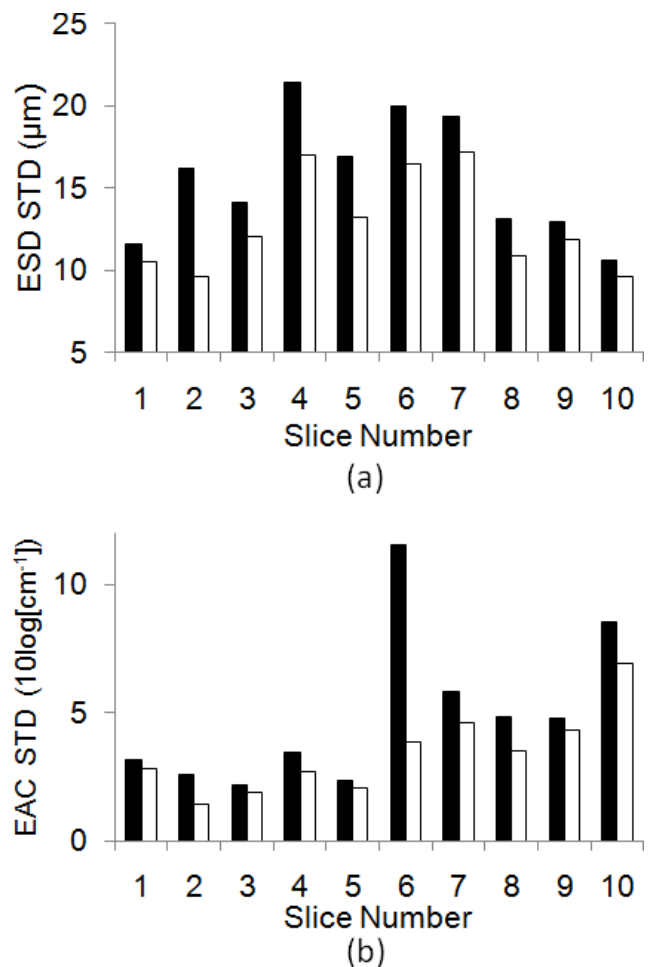


Figure 2. (a) ESD standard deviations when including specular scatterers (black) and when excluding specular scatterers (white). (b) EAC standard deviations when including specular scatterers (black) and when excluding specular scatterers (white).

A total of six fresh beef liver samples were included in the temperature monitoring analysis. Fig. 3 includes ESD and EAC mean curves as a function of temperature for the beef liver samples when including specular scatterers. In contrast, Fig. 4 includes ESD and EAC mean curves as a function of temperature for the beef liver samples when excluding specular scatterers. By excluding the specular scatterers, ESD and EAC mean were observed to change by 25.4% and -40.3% respectively as opposed to 14.8% and -30.7% respectively when including specular scatterers.

IV. DISCUSSION

Two effects were observed for the simulated backscatter data when excluding specular scatterers compared to including specular scatterers. First, the standard deviation of the collection of estimates was significantly reduced, resulting in increased precision. Second, the ESD mean value was more accurate in estimating the simulated diffuse scatterer size than the ESD mean value estimated when including specular

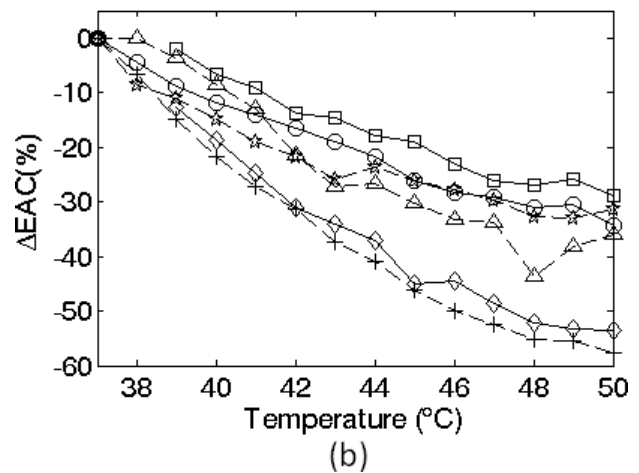
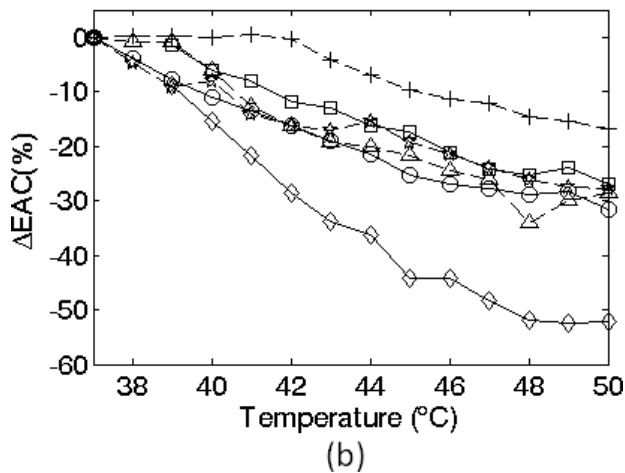
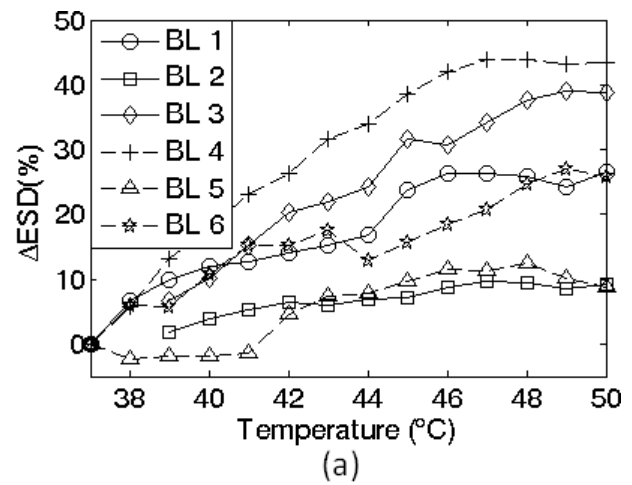
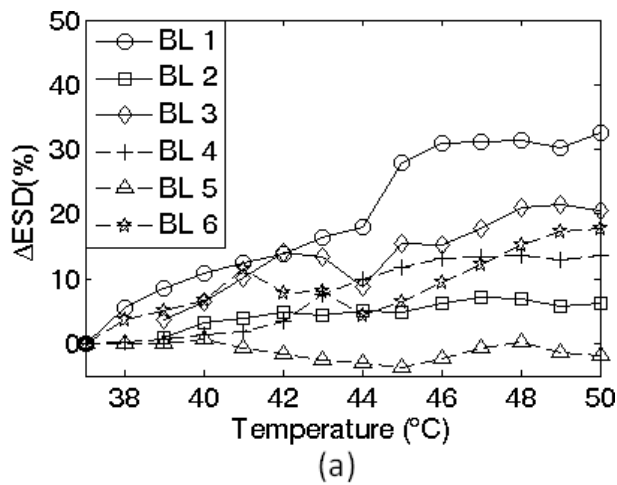


Figure 3. Beef liver tissue samples. Change in (a) ESD and (b) EAC as a function of temperature when specular scatterers are included.

Figure 4. Beef liver tissue samples. Change in (a) ESD and (b) EAC as a function of temperature when specular scatterers are excluded.

scatterers. These results suggest that it may be possible to create QUS parametric images based on diffuse scattering only.

For the rat mammary tumors, excluding specular scatterers from the analysis resulted in reductions of ESD and EAC standard deviations for all tumors. The tumors that exhibited the greatest reduction in ESD and EAC standard deviation also had the greatest number of specular scatterers. For the beef liver samples, excluding specular scatterers from QUS analysis resulted in larger changes in the ESD and EAC mean for increases in temperatures compared to including specular scatterers.

V. CONCLUSION

When data blocks containing only diffuse scatterers were included in QUS analysis, the precision of QUS estimates was improved and larger changes in QUS parameters were observed for temperature elevation. These results suggest that the GS intercept parameter has the potential to improve QUS imaging by reducing the effects of specular scatterers on diffuse scattering estimates.

ACKNOWLEDGMENT

The authors would like to thank Ellora Sen-Gupta, Andrew Battles, Mikey Tu, and Zachary T. Hafez for collecting the rat mammary tumor data used in this paper.

REFERENCES

- [1] M. L. Oelze, W. D. O'Brien, Jr., J. P. Blue, and J. F. Zachary, "Differentiation and characterization of rat mammary fibroadenomas and 4T1 mouse carcinomas using quantitative ultrasound imaging," *IEEE Trans. on Med. Imag.*, vol. 23, pp. 764-771, June 2004.
- [2] E. J. Feleppa, F. L. Lizzi, D. J. Coleman and M. M. Yaremko, "Diagnostic spectrum analysis in ophthalmology: A physical perspective," *Ultrasound in Med. & Biol.*, vol. 12, pp. 623-631, 1986.
- [3] E. J. Feleppa, T. Liu, A. Kalisz, M. C. Shao, N. Fleshner, V. Reuter, and W. R. Fair, "Ultrasonic spectral-parameter imaging of the prostate," *Int. J. Imaging Syst. Technol.*, vol. 8, pp. 11-25, 1997.
- [4] K. D. Donohue, L. Huang, T. Burks, F. Forsberg, and C. W. Piccoli, "Tissue classification with generalized spectrum parameters," *Ultrasound in Med. & Biol.*, vol. 27, no. 11, pp. 1505-1514, 2001.
- [5] M. F. Insana, R. F. Wagner, D. G. Brown, and T. J. Hall, "Describing small-scale structure in random media using pulse-echo ultrasound," *J. Acoust. Soc. Am.*, vol. 87, pp. 179-192, January 1990.